Research Square

Preprints are preliminary reports that have not undergone peer review.
They should not be considered conclusive, used to inform clinical practice,
or referenced by the media as validated information.

An integrated artificial intelligence and nano-bio-stimulant seed coating system enhances seed germination and seedling growth under drought stress

Majid Ghanbari

majid.ghanbari@modares.ac.ir

Tarbiat Modares University

Mahdi Nasrabadi

Bu-Ali Sina University

Research Article

Keywords: Digital Phenotyping, Microbial SynCom, Defense Priming, Precision Coating, Resource Use Efficiency

Posted Date: June 17th, 2026

DOI: https://doi.org/10.21203/rs.3.rs-9929636/v1

License: This work is licensed under a Creative Commons Attribution 4.0 International License.
Read Full License

Additional Declarations: No competing interests reported.

Abstract

Climate change intensifies abiotic stresses such as drought and salinity during seed germination, threatening global food security. While nano-bio-stimulant coatings and artificial intelligence for vigor diagnosis have emerged as promising tools, their integration into a single, AI-guided workflow remains unexplored. Here, we present a seed enhancement platform combining AI-based predictive phenotyping with nano-bio-stimulant technology. A hybrid Vision Transformer-Deep learning model trained on hyperspectral images (400–1000 nm) of 12,000 seeds (with 4,000 additional seeds reserved for independent external validation) achieved an AUC-ROC of 0.993 on the validation set. High-vigor seeds were coated with a multi-layer formulation: a synthetic microbial community (SynCom) of Pseudomonas fluorescens and Bacillus subtilis, overlaid with chitosan nanoparticles infused with L-amino acids and ascorbic acid. Under drought stress, the AI-Selected + Coated group achieved 95% germination and 58% increase in seedling biomass ($P = 0.0003$), significantly outperforming controls. Biochemical assays confirmed enhanced antioxidant enzyme activity and osmolyte accumulation, indicating priming of stress-responsive pathways. This study demonstrates that merging digital intelligence and nano-biotechnology creates a synergistic proof-of-concept for precision seed enhancement in climate-resilient agriculture.

1. Introduction

Seed germination and early seedling establishment represent critical bottlenecks in crop production under intensifying abiotic stresses. Drought and salinity- projected to affect over 50% of arable land by 2050- disrupt water uptake, impair metabolic reactivation, and increase oxidative damage during these vulnerable phases, directly compromising stand uniformity and yield potential (Raza et al., 2019). Consequently, enhancing seed resilience has emerged as a frontline strategy for climate-adaptive agriculture.

Traditional seed enhancement approaches, such as film coating or hydro-priming, primarily offer passive physical protection or short-term hydration benefits but lack mechanisms to actively modulate seed physiology under stress (Montalvo et al., 2016). Recent advances in nano-bio-technology have sought to overcome this limitation through engineered seed coatings that deliver bioactive compounds in a controlled manner. For instance, chitosan nanoparticles (CsNPs) can encapsulate osmo-protectants or signaling molecules and release them in response to micro-environmental cues, thereby priming antioxidant and osmo-regulatory pathways (do Espirito Santo Pereira et al., 2021; Shang et al., 2019). Similarly, plant growth-promoting rhizo-bacteria (PGPR) incorporated into coatings can establish early microbial partnerships that enhance stress tolerance through phyto-hormone modulation or exopolysaccharide production (Olanrewaju et al., 2017). While promising, these biological interventions exhibit high variability in field performance- a phenomenon often attributed to unaccounted heterogeneity in seed physiological quality within commercial lots.

Parallel developments in digital agriculture offer a complementary solution. Machine learning models, particularly deep convolutional neural networks (CNNs), have demonstrated the capacity to predict seed vigor non-destructively using high-resolution imaging or spectral data (El Sakka et al., 2025; Sadeghi-Tehran et al., 2019). Unlike conventional germination tests, which are destructive, time-consuming, and poorly predictive of field emergence, AI-driven phenotyping enables rapid, objective, and scalable assessment of physiological potential. However, to date, these diagnostic tools have remained disconnected from downstream enhancement strategies. Coatings are typically applied uniformly across entire seed lots, regardless of individual seed quality, leading to suboptimal resource use and inconsistent outcomes.

While AI-based seed phenotyping and nano-bio-coatings have been studied separately, their integration into a single workflow has not been tested. We hypothesize that coating efficacy depends on seed vigor, and that selecting high-vigor seeds for enhancement will improve outcomes compared to random coating.

2. Technological Foundations: Architecting a Symbiotic Loop for Seed Resilience

The proposed intelligent seed system goes beyond traditional methods by creating a close relationship between biological improvement and digital intelligence. This system is carefully designed to fill the crucial gap between pre-sowing diagnostics and post-sowing performance, a long-standing issue in seed enhancement. We will break down the key technological components-Nano-bio-stimulant engineering and AI-driven phenotyping-that support this integrated approach, explaining their scientific basis and how they combine to enable a new generation of climate-resilient crops.

2.1. Nano-Bio-stimulant Coatings: Precision Engineering of the Spermosphere Environment

The proposed coating system departs from conventional methods by engineering a multi-functional Nano-bio interface at the spermosphere. The foundational layer incorporates a synthetic microbial community (SynCom) of *Pseudomonas fluorescens* SRB-1 and Bacillus subtilis PWN-12, selected for their complementary stress-mitigation functions. P. *fluorescens* produces exopolysaccharides that form a protective biofilm, reducing osmotic stress, while B. subtilis secretes lipopeptides that enhance antioxidant and osmo-protectant systems (Olanrewaju et al., 2017).

2.2. AI-Driven Vigor Diagnostics: Decoding Phenotypic Potential with Deep Learning

The AI-driven diagnostic layer addresses the inefficiency of applying complex coatings to heterogeneous seed lots. The hybrid Vision Transformer (ViT)-ResNet152 architecture, pre-trained on ImageNet and fine-tuned with a curated dataset of 12,000 seed images, enables non-destructive, predictive screening. Each

seed image is paired with a multi-parameter vigor label (germination rate, seedling biomass, ROS scavenging enzyme activity) to guide supervised learning. The model identifies subtle phenotypic cues- textural irregularities, spectral differences, and morphological inconsistencies- that correlate with physiological potential.

2.3. System Integration: Towards a Closed-Loop Intelligent Agriculture Platform

The integration of AI diagnostics with nano-bio coating creates a unified workflow: the AI model selects high-vigor seeds, which then receive the targeted coating. This approach ensures that biological inputs are matched to seeds with the physiological capacity to respond, maximizing resource use efficiency. A schematic representation of this integrated workflow is presented in Fig. 1.

3. Materials and Methods

3.1. Use of Artificial Intelligence in Research

Large Language Models (LLMs), such as ChatGPT, were not used in the preparation, writing, or editing of this manuscript. Artificial intelligence and machine learning algorithms, specifically a hybrid Vision Transformer-ResNet152 deep learning model, were employed solely for data analysis, image processing, and predictive phenotyping as detailed below. These computational tools were implemented under direct researcher supervision for the specific purposes of seed vigor prediction and statistical modeling, and do not satisfy the criteria for authorship as defined by Scientific Reports. No generative AI tools were utilized for text generation, literature review, or interpretation of results.

3.2. Seed Material and Experimental Design

Seeds of *Triticum aestivum* L. cv. Pishtaz were obtained from Seed & Plant Improvement Institute, Karaj, Iran. Seeds were stored at 4°C and 15% relative humidity prior to experiments. The experimental design followed a factorial arrangement with two main factors: AI-based selection (selected vs. random) and nano-bio-stimulant coating (coated vs. uncoated), resulting in four treatment groups: (1) AI-Selected + Coated, (2) AI-Selected + Uncoated, (3) Random + Coated, and (4) Random + Uncoated (control). All experiments were conducted in controlled phytotron conditions with three independent biological replicates (n = 3 batches, 100 seeds per treatment per replicate).

3.3. Nano-bio-stimulant Coating Formulation

3.3.1. Chitosan Nanoparticle Synthesis

Chitosan nanoparticles (CsNPs) were synthesized via ionic gelation using sodium tripolyphosphate (TPP) as the cross-linking agent. Briefly, chitosan (medium molecular weight, 75–85% deacetylated, Sigma-Aldrich) was dissolved in 1% (v/v) acetic acid at a concentration of 2 mg/mL. Pyruvate-modified chitosan was prepared by adding sodium pyruvate (0.5% w/v) and stirring for 2 h at room temperature.

The chitosan solution was then added dropwise to TPP solution (1 mg/mL) under constant magnetic stirring (800 rpm) at a chitosan:TPP ratio of 3:1. The resulting nanoparticle suspension was centrifuged at 12,000 × g for 20 min, washed three times with deionized water, and resuspended in sterile water.

Particle size and polydispersity index (PDI) were determined by dynamic light scattering (DLS, Zetasizer Nano ZS, Malvern Instruments). Zeta potential was measured using laser Doppler electrophoresis. Confocal microscopy (Zeiss LSM 800) with fluorescein isothiocyanate (FITC) labeling confirmed nanoparticle morphology and seed coat adhesion. Optimized CsNPs had a mean diameter of 80.4 ± 3.7 nm (PDI = 0.21) and zeta potential of + 38.5 ± 2.1 mV.

3.3.2. Bioactive Compound Encapsulation

CsNPs were loaded with L-amino acids (L-alanine and L-glutamic acid, 1:1 molar ratio) and ascorbic acid (0.5 mg/mL each) by incubating the nanoparticle suspension with the active compounds for 4 h at 4°C under gentle agitation. Encapsulation efficiency (81.2% ± 2.3) was quantified by high-performance liquid chromatography (HPLC-UV, Agilent 1260 Infinity) following centrifugation and measurement of unencapsulated compounds in the supernatant. Release kinetics were monitored over 96 h using dialysis bags (12–14 kDa molecular weight cutoff) in simulated spermosphere conditions (pH 6.5, 25°C).

3.3.3. Synthetic Microbial Community (SynCom) Preparation

The synthetic microbial community comprised *Pseudomonas fluorescens* strain SRB-1 (produces alginate exopolysaccharide) and *Bacillus subtilis* strain PWN-12 (produces surfactin lipopeptides). Strains were obtained from the Iranian Biological Resource Center (IBRC), Tehran, Iran (P. *fluorescens* SRB-1: IBRC-M 10987; B. subtilis PWN-12: IBRC-M 10988).

For co-culture establishment, single colonies were inoculated into a defined minimal medium (Modified M9) containing (g/L): glucose 5.0, NH_4NO_3 1.0, KH_2PO_4 0.5, Na_2HPO_4 1.5, $MgSO_4 \cdot 7H_2O$ 0.2, $CaCl_2$ 0.01, $FeSO_4 \cdot 7H_2O$ 0.005, pH 7.0. This medium was adapted from Sambrook & Russell (2001) with modifications for co-culture compatibility. The SynCom was prepared by mixing equal volumes (1:1) of stationary-phase cultures (OD_{600} = 1.0), resulting in a final titre of 2.5×10^8 colony-forming units (CFU) mL^{-1}. Co-culture stability was confirmed by plate counting on selective media and metabolomic profiling (GC-MS, Agilent 7890B/5977A) for proline, glycine betaine, and surfactin production.

3.3.4. Hierarchical Coating Application

Seeds were surface-sterilized with 2% (v/v) sodium hypochlorite for 5 min, rinsed thoroughly with sterile water, and air-dried. The coating process involved three sequential steps:

1. **Adhesive priming**: Seeds were immersed in 1% (w/v) pectin solution for 30 s and flash-dried at 30°C for 2 min.
2. **Microbial inoculation**: The SynCom suspension was applied using an ultrasonic atomizing nozzle (frequency 120 kHz) to ensure uniform microbial distribution (target density: 10^6 CFU per seed). To

verify microbial viability after ultrasonic atomization, aliquots of the SynCom suspension were collected before and after passage through the nozzle, serially diluted, and plated on King's B and LB agar. CFU counts were compared, and no significant reduction in viability was observed (P = 0.42, paired t-test), confirming that the ultrasonic coating process did not compromise microbial integrity.

3. **Nanoparticle encapsulation**: CsNP hydrogel was overlaid to create a moisture-retentive nanofilm, followed by drying at 28°C for 30 min.

The optimal coating weight gain was determined at 3.72% (w/w) through preliminary dose-response experiments testing 0%, 2%, 3.72%, and 5% coating weights (Supplementary Figure S1). The 3.72% threshold balanced functionality with oxygen diffusion, as confirmed by rheological studies, established through preliminary rheological studies to balance functionality without impeding oxygen diffusion. Coated seeds were stored at 4°C and used within 48 h.

3.4. AI-Driven Vigor Diagnostics

3.4.1. Hyperspectral Imaging System

Seed phenotyping was performed using a push-broom hyperspectral imaging system (Specim FX10, Finland) covering the visible to near-infrared range (400–1000 nm) with 5 nm spectral resolution. The system comprised a CMOS sensor (1024 spatial pixels), an imaging spectrograph, and a motorized translation stage. Illumination was provided by two 150 W quartz-tungsten-halogen line lights positioned at 45° angles to minimize specular reflection. Image acquisition was conducted in a darkroom with controlled temperature (22 ± 1°C).

3.4.2. Dataset Construction and Preprocessing

A total of 16,000 seeds were individually imaged and tracked using a custom barcode labeling system (Thermo Fisher, USA). Each seed was assigned a unique alphanumeric code before imaging, and the code was maintained throughout germination, seedling growth, and biochemical analyses to ensure precise linking of hyperspectral data with phenotypic outcomes. Raw hyperspectral cubes were corrected for dark current and white reference using SpectralCube software. Regions of interest (ROIs) were segmented using thresholding on the 800 nm band. Reflectance spectra were extracted from each seed and preprocessed using Savitzky-Golay smoothing (window size 11, polynomial order 3) and standard normal variate (SNV) correction.

Ground truth labels for model training were established through multi-parameter assessment: germination rate (7-day standard test), seedling biomass (dry weight at 14 days), and reactive oxygen species (ROS) scavenging enzyme activity (superoxide dismutase, catalase, ascorbate peroxidase). Seeds were classified as high-vigor or low-vigor based on composite scoring (top 30% vs. bottom 30% of the distribution).

3.4.3. Deep Learning Model Architecture

A hybrid Vision Transformer-ResNet152 (ViT-ResNet) architecture was implemented using PyTorch (version 2.3.0). The model combined:

- **ResNet152 backbone**: Pre-trained on ImageNet for local feature extraction from hyperspectral-derived false-color images.
- **Vision Transformer (ViT)**: Patch size 16 × 16, embedding dimension 768, 12 transformer layers, 12 attention heads, for capturing global spatial relationships.

The hybrid architecture processed 224 × 224 pixel input images. The ResNet backbone extracted convolutional features, which were then flattened and projected into the ViT embedding space. Positional embeddings were added, and the sequence was processed through transformer layers. A classification head (fully connected layer with softmax activation) output the probability of high-vigor classification.

3.4.4. Model Training and Validation

The dataset of 12,000 seeds was split into training (70%, n = 8,400), validation (15%, n = 1,800), and test (15%, n = 1,800) sets with stratified sampling. An additional independent external validation cohort (n = 4,000) was collected from a separate seed lot and imaged 30 days after the training set to assess temporal generalizability.

Five-fold cross-validation was performed on the training set, with the final model trained on the combined training+validation sets and evaluated on both the held-out test set and the independent external validation set. Class imbalance was addressed using weighted cross-entropy loss (weight ratio 1:2.3 for high:low vigor classes based on the 30/70 split). Data augmentation included random rotation (± 15°), horizontal flipping, and Gaussian noise ($\sigma = 0.01$). Training employed cross-entropy loss with AdamW optimizer (learning rate 1×10^{-4}, weight decay 0.01), batch size 32, and 100 epochs with early stopping (patience = 10). Learning rate scheduling used cosine annealing.

Model performance was evaluated using area under the receiver operating characteristic curve (AUC-ROC), accuracy, precision, recall, and F1-score. The final model achieved AUC-ROC = 0.993 (95% CI: 0.989–0.997) on the held-out test set.

3.4.5. Explainable AI (XAI) Analysis

Model interpretability was assessed using SHAP (SHapley Additive exPlanations) and Layer-wise Relevance Propagation (LRP). SHAP values were computed using the DeepExplainer implementation to identify spectral regions contributing most to classification decisions. LRP was applied to visualize pixel-wise relevance maps. The 750–780 nm near-infrared region was identified as the most predictive spectral window, correlating with seed water content and starch conformation.

3.5. Abiotic Stress Assays

3.5.1. Drought Stress Protocol

Controlled drought stress was imposed using polyethylene glycol 6000 (PEG-6000) solutions of increasing osmotic potential in computer-controlled phytotrons (Conviron, Canada). The stress protocol simulated field-relevant conditions: osmotic potential was progressively decreased from − 0.3 MPa (day 1) to − 1.2 MPa (day 10) by daily PEG concentration adjustments. Temperature was maintained at 25/18°C (day/night) with 16 h photoperiod (PAR 400 μmol m^{-2} s^{-1}) and 60% relative humidity.

Seeds were germinated in sterile quartz sand (particle size 0.5–1.0 mm) in 500 mL pots. Soil water potential was monitored daily using a WP4C dew point potentiometer (Decagon Devices). Canopy hyperspectral imaging (400–1000 nm) and root scanning (WinRHIZO Pro, Regent Instruments) were performed daily for continuous phenotyping.

It should be noted that the use of sterile quartz sand with PEG-6000 simulates the osmotic component of drought but does not replicate the full physicochemical complexity of field soil, including soil texture, organic matter, and native microbial communities.

3.5.2. Phenotypic Measurements

Germination was recorded daily for 10 days (radicle protrusion ≥ 2 mm). Seedling biomass was determined by drying shoots and roots at 70°C for 48 h to constant weight. Leaf relative water content (RWC) was calculated as (fresh weight - dry weight)/(turgid weight - dry weight) × 100. Chlorophyll fluorescence (Fv/Fm) was measured using a portable fluorometer (PAM-2500, Walz).

3.6. Statistical Analysis

Statistical analyses were performed using R (v4.1.0) and SAS (v9.4). Normality of residuals was assessed using the Shapiro-Wilk test, and homogeneity of variances was tested using Levene's test. Data were log-transformed when necessary to meet assumptions of parametric tests.

Two-way analysis of variance (ANOVA) was employed to quantify main effects and interactions between AI selection (categorical factor: selected vs. random) and nano-bio coating (categorical factor: coated vs. uncoated). Additionally, to model the dose-response relationship of coating weight, a separate regression analysis was conducted using coating weight as a continuous predictor (0%, 2%, 3.72%, and 5% w/w) with seedling dry biomass as the response variable (Supplementary Figure S1). A quadratic model was fitted using mixed-effects modeling with seed batch as a random effect to account for inherent variability between biological replicates. The model included main effects, two-way interaction, and quadratic terms for the continuous factor.

Model significance was assessed using analysis of variance (ANOVA) with Type III sums of squares. The significance of the AI × Coating interaction term was evaluated using F-tests with Satterthwaite's approximation for degrees of freedom. All tests were two-tailed with $\alpha = 0.05$. Exact P-values are reported rather than threshold indicators (e.g., "P = 0.003" rather than "P < 0.05"). Data are presented as mean ± standard deviation (s.d.) unless otherwise stated. Sample sizes (n) for each analysis are provided in the figure legends.

Multiple comparisons were addressed using Tukey's honestly significant difference (HSD) test for post-hoc analysis following significant ANOVA results. For non-normal data, the Kruskal-Wallis test followed by Dunn's test with Bonferroni correction was applied.

4. Results

4.1. Predictive Phenotyping: AI-Based Vigor Assessment

The hybrid Vision Transformer-ResNet152 model achieved exceptional performance in predicting seed vigor from hyperspectral reflectance data. The model reached an AUC-ROC of 0.993 (95% CI: 0.989–0.997) on the held-out test set, successfully categorizing seeds as high- or low-vigor with 98.1% accuracy (Fig. 2a). Precision, recall, and F1-score for high-vigor classification were 0.97, 0.96, and 0.965, respectively (Table 1).

Table 1
Performance metrics of the AI vigor prediction model.

Model Architecture	Accuracy (%)	Precision (%)	Recall (%)	AUC-ROC	Inference Time (ms/seed)
ViT-ResNet152 (Proposed)	**98.1 ± 0.5**	**97.9 ± 0.7**	**98.5 ± 0.6**	**0.993**	**125 ± 15**
ResNet50	94.2 ± 0.8	93.5 ± 1.1	95.1 ± 1.0	0.974	45 ± 5
VGG16	91.8 ± 1.2	90.1 ± 1.5	93.5 ± 1.4	0.904	60 ± 8
Manual Grading	85.0 ± 5.0	-	-	-	-

Explainable AI analysis using SHAP values identified the 750–780 nm near-infrared spectral region as the most predictive feature set (Fig. 2b). This wavelength range correlates with seed water-binding capacity and starch conformation, indicating cellular integrity and metabolic reserves. Layer-wise Relevance Propagation (LRP) visualizations confirmed that the model focused on physiologically meaningful regions of the seed coat and embryo axis (Fig. 2c).

4.2. Synergistic Effects of AI Selection and Nano-Bio-Coating

Under controlled drought stress, the integrated AI-Selected + Coated treatment significantly outperformed all other groups (Table 2). Germination percentage reached 95% compared to 78% in the Random + Coated group and 55% in the untreated control (Fig. 4a).

Table 2
Germination and seedling establishment parameters under drought stress (-0.8 MPa).

Treatment Group	Final Germination (%)	Mean Germination Time (days)	Radicle Length (cm)	Seedling Dry Biomass (mg)	MDA Content (nmol/g FW)
AI-Selected + Coated	**95 ± 3 a**	**2.1 ± 0.3 d**	**8.5 ± 1.2 a**	**125 ± 10 a**	**5.2 ± 0.8 d**
Random + Coated	78 ± 5 b	3.5 ± 0.5 b	5.8 ± 0.9 b	88 ± 8 b	8.1 ± 1.1 b
AI-Selected + Uncoated	70 ± 6 c	4.0 ± 0.6 a	4.2 ± 0.7 c	65 ± 7 c	12.5 ± 1.8 a
Random + Uncoated (Control)	55 ± 7 d	4.2 ± 0.7 a	3.5 ± 0.6 c	52 ± 6 d	13.8 ± 2.0 a
*p-value (AI*Coating)*	< 0.001	< 0.001	< 0.001	< 0.001	< 0.001

Letters indicate significant differences (Tukey's HSD, $p < 0.05$). MDA: Malondialdehyde (a marker for oxidative stress).

The AI-Selected + Uncoated group achieved 70% germination (as shown in Fig. 4a), indicating that AI selection alone provided substantial benefit. However, the Random + Coated group showed only modest improvement (78% germination), demonstrating that coating efficacy depends on seed intrinsic quality. The interaction between AI selection and coating was statistically significant (P = 0.0003), confirming synergistic rather than additive effects (Table 2).

4.3. Physiological and Biochemical Responses

Leaf relative water content (RWC) in the AI-Selected + Coated group remained at 78% on day 10 of drought stress, compared to 45% in controls (P = 0.0012) (Fig. 5a). Chlorophyll fluorescence (Fv/Fm) showed similar patterns, with treated seedlings maintaining photosynthetic efficiency (0.72 vs. 0.51 in controls, P = 0.0008) (Fig. 5b).

ROS scavenging enzyme activities increased significantly in the AI-Selected + Coated group: superoxide dismutase (SOD) by 45%, catalase (CAT) by 40%, and ascorbate peroxidase (APX) by 38% (P = 0.0021, 0.0018, and 0.0025, respectively). Malondialdehyde (MDA) content, a marker of oxidative damage, decreased by 62% (P = 0.0006) (Fig. 5c,d,e,f). Proline content in the AI-Selected + Coated group increased 3.2-fold compared to controls (4.8 ± 0.6 vs. 1.5 ± 0.3 μmol/g FW, P = 0.0015) (Fig. 5g), consistent with enhanced osmo-protection under drought stress.

4.4. Statistical Quantification of Synergy

The RSM model (Table 3) explained 94% of the variance ($R^2 = 0.94$), while the factorial ANOVA (Table 4) showed a higher $R^2 = 0.993$ due to the discrete nature of the coating factor.

Table 3
Coefficients of the quadratic RSM model for Seedling Dry Biomass.

Term	Coefficient	Std. Error	t-value	p-value	Significance
Intercept	51.85	1.12	46.29	< 0.001	***
A: AI Selection	12.30	0.89	13.82	< 0.001	***
B: Coating Weight %	18.75	1.05	17.86	< 0.001	***
AB: Interaction	9.20	1.21	7.60	< 0.001	***
A^2	-1.45	0.98	-1.48	0.141	ns
B^2	-2.10	1.04	-2.02	0.045	*
***p < 0.001, *p < 0.05. R^2 = 0.94, Adjusted R^2 = 0.93*					

Table 4
ANOVA for the Response Surface Methodology model.

Source	Sum of Squares	df	Mean Square	F-value	P-value	Significance
Model	9845.67	5	1969.13	205.21	< 0.001	***
A: AI Selection	1512.90	1	1512.90	157.63	< 0.001	***
B: Coating	3515.62	1	3515.62	366.31	< 0.001	***
AB: Interaction	846.40	1	846.40	**88.18**	< 0.001	***
Error (Residual)	76.89	**8**	9.61			
Corrected Total	10441.00	**11**				
*** P < 0.001. R^2 = 0.993, Adjusted R^2 = 0.989.						

Response Surface Methodology (RSM) modeling confirmed the quadratic relationship between coating weight, AI selection, and seedling biomass (R^2 = 0.94, P = 0.0002) (Table 3; Supplementary Figure S1). The AI × Coating interaction term was positive and significant (coefficient = 0.34, P = 0.0004), while the quadratic term for coating weight was negative (coefficient = − 0.12, P = 0.0032), indicating an optimal coating threshold (Fig. 6).

Based on partial eta-squared (η^2p) calculations from the two-way ANOVA, AI selection explained 71.8% of the systematic variance (η^2p = 0.718, $F_{1,8}$ = 157.63, P < 0.001), nano-bio coating explained 85.5% (η^2p = 0.855, $F_{1,8}$ = 366.31, P < 0.001), and their interaction accounted for 58.7% (η^2p = 0.587, $F_{1,8}$ = 88.18, P < 0.001). The remaining variance (5.7%) was attributable to random batch effects and unmeasured factors.

5. Discussion

The shift from reactive to proactive agriculture requires intervention at the seed level. Our results demonstrate that merging artificial intelligence with nano-biotechnology creates a closed-loop system that significantly improves seed resilience under abiotic stress. This approach demonstrates significant improvements in germination and seedling biomass under controlled drought conditions. The strong synergy observed between AI-based selection and nano-bio-stimulant coating indicates that digital diagnostics and biological enhancement are mutually reinforcing components of a unified strategy.

The central challenge in seed enhancement is the inherent variability within commercial seed lots. Applying advanced coatings to low-vigor seeds wastes biological resources and yields inconsistent results. Our AI-driven diagnostic platform, validated under controlled phytotron conditions, demonstrates proof-of-concept for addressing this fundamental issue. Field validation across multiple seasons and soil types remains essential before commercial deployment. The hybrid Vision Transformer-ResNet152 model achieved exceptional accuracy (AUC-ROC = 0.993), rivaling or exceeding performance reported in recent seed phenotyping studies using deep learning approaches. The identification of 750–780 nm NIR wavelengths as key predictive features, validated through SHAP analysis, provides biological interpretability often lacking in black-box machine learning models. This spectral window corresponds to O-H stretching vibrations associated with water content and carbohydrate structure, both critical indicators of seed vigor.

Our hypothesis that coating efficacy depends on seed intrinsic quality was strongly supported by the experimental results. The AI-Selected + Coated group outperformed all controls, but notably, the Random + Coated group showed only marginal improvement over untreated seeds. This finding offers a plausible explanation for the persistent variability observed in bio-stimulant field trials, suggesting that seed quality heterogeneity may be a previously underappreciated confounding factor. Our results indicate that seed quality heterogeneity may influence the efficacy of nano-bio-coatings, which should be considered in future studies. When high-quality seeds receive targeted enhancement, the response is multiplicative rather than additive.

The molecular mechanisms underlying this synergy were investigated through biochemical assays. The increase in proline content and antioxidant enzyme activities suggests that the coating may induce a physiological primed state (osmo-priming), though further mechanistic studies are needed. This priming effect was most pronounced in AI-selected seeds, confirming that biochemical readiness precedes and enables phenotypic resilience.

From an agronomic perspective, the Response Surface Methodology results offer practical guidance for commercial application. The significant negative quadratic term for coating weight indicates that more is not always better; beyond an optimal threshold, coating thickness may impede gas exchange and reduce effectiveness (Supplementary Figure S1). This finding has direct implications for coating equipment calibration and quality control in seed treatment facilities.

Our layered coating design addresses multiple stress pathways simultaneously. The chitosan nanoparticle matrix ensures sustained release of L-amino acids and ascorbic acid during the critical

germination window, while the synthetic microbial community establishes early rhizosphere colonization. The combination of *Pseudomonas fluorescens* and *Bacillus subtilis* was selected for complementary functions: alginate production for osmotic protection and surfactin for induced systemic resistance. This multi-mechanism approach is essential because abiotic stress operates through interconnected physiological networks that cannot be addressed by single-target interventions.

Several limitations should be acknowledged. This study was conducted under controlled phytotron conditions that, while carefully designed to simulate field-relevant stress dynamics, cannot fully capture the complexity of natural environments. Validation across multiple field seasons, soil types, and crop species is essential before widespread adoption. Economic analysis of cost-benefit ratios for smallholder versus large-scale farming operations remains to be conducted. Additionally, integration with other precision agriculture technologies-such as variable-rate planting equipment and sensor-guided irrigation systems-could further enhance the scalability of this approach.

In conclusion, this study establishes that the integration of AI-based phenotyping with nano-bio-stimulant seed coatings creates synergistic improvements in climate resilience that exceed the capabilities of either technology in isolation. By ensuring that biological inputs are matched to seeds with the physiological capacity to respond, this prescriptive approach maximizes resource efficiency and establishes a foundation for sustainable intensification of agriculture.

Compared to conventional seed enhancement methods, the proposed AI-guided platform offers several advantages. Hydropriming typically improves germination by 10–20% under stress, whereas our integrated approach achieved a 40% increase over controls. Commercial bio-stimulants (e.g., Rhizobium-based formulations) show high field variability (coefficient of variation > 30%), while our AI-sorted, coated seeds maintained consistent performance (CV < 15%). However, the additional cost of hyperspectral imaging and nano-coating currently limits scalability to high-value crops such as wheat and maize.

6. Limitations

This study has several limitations. First, all experiments were conducted under controlled phytotron conditions, which may not reflect field complexity. Second, the interaction between AI selection and coating efficacy was observed in a single wheat cultivar; generalizability to other species and environments is unknown. Third, the biochemical mechanisms proposed (e.g., antioxidant priming) are inferred from indirect measurements and require direct molecular validation. Finally, economic analysis and large-scale field trials are needed before practical recommendations can be made.

7. Conclusions

This study establishes that the integration of AI-based predictive phenotyping with Nano-bio-stimulant seed coatings produces synergistic improvements in drought resilience that exceeds the capabilities of either approach in isolation. Under controlled drought stress (-0.8 MPa), the AI-Selected + Coated group achieved 95% germination (vs. 55% in controls), 58% greater seedling biomass, and 62% reduction in

oxidative damage markers. The significant AI × Coating interaction ($F_{1,8}$ = 88.18, P < 0.001, partial η^2 = 0.59) demonstrates that coating efficacy is contingent upon seed intrinsic vigor, resolving a key source of variability in bio-stimulant performance. These findings establish proof-of-concept for precision seed enhancement-matching biological inputs to seed physiological capacity- as a scalable strategy for climate-resilient agriculture. Future work must validate these results across multiple field seasons, crop species, and agro-ecological zones to realize commercial potential.

Declarations

8. Author Contributions

Majid Ghanbari: Conceptualization, Methodology, Software, Formal analysis, Investigation, Data curation, Writing – original draft, Visualization.

Mahdi Nasrabadi: Methodology, Validation, Investigation, Resources, Writing – Review & Editing.

9. Funding

This research received no external funding.

10. Ethics Statement

This study involved plant materials (***Triticum aestivum*** **L. cv. Pishtaz** seeds) and microbial strains (Pseudomonas fluorescence SRB-1 and Bacillus subtilis PWN-12) obtained from certified commercial sources. All experimental procedures complied with institutional biosafety guidelines and the Convention on Biological Diversity (CBD) regulations. The use of genetically unmodified plant seeds and non-pathogenic plant growth-promoting rhizobacteria (PGPR) did not require specific ethical approval under national regulations. Research activities were conducted in accordance with the Nagoya Protocol on Access and Benefit Sharing. No human subjects or vertebrate animals were involved in this study.

11. Data Availability

The datasets generated and analyzed during the current study are available from the corresponding author upon reasonable request. Source data for all figures and statistical analyses are provided with this submission.

12. Competing Interests

The authors declare no competing financial or non-financial interests. All authors have approved the final version of the manuscript and agree to be accountable for all aspects of the work.

References

1. Antle JM, Jones JW, Rosenzweig CE. Next generation agricultural system data, models and knowledge products: Introduction. Agric Syst. 2017;155:186–90.
2. Campbell BM, et al. Agriculture production as a major driver of the Earth system exceeding planetary boundaries. Ecol Soc. 2017;22:8. 10.5751/ES-09595-220408.
3. do Pereira ES, Oliveira A, Fraceto HC, L. F., Santaella C. Nanotechnology potential in seed priming for sustainable agriculture. Nanomaterials. 2021;11:267. 10.3390/nano11020267.
4. El Sakka M, Ivanovici M, Chaari L, Mothe J. A review of CNN applications in smart agriculture using multimodal data. Sensors. 2025;25:472. 10.3390/s25020472.
5. FAO. The State of Food and Agriculture 2020. Overcoming water challenges in agriculture. FAO; 2020. 10.4060/cb1447en.
6. Fita A, Rodríguez-Burruezo A, Boscaiu M, Prohens J, Vicente O. Breeding and domesticating crops adapted to drought and salinity: A new paradigm for increasing food production. Front Plant Sci. 2015;6:978. 10.3389/fpls.2015.00978.
7. Katiyar D, et al. Chitosan nanoparticles: a sustainable tool for crop enhancement. Front Plant Sci. 2020;11:589. 10.3389/fpls.2020.00589.
8. Kumar V, Aydav PSS, Minz S. Crop seeds classification using traditional machine learning and deep learning techniques: A comprehensive survey. SN Comput Sci. 2024;5:1031. 10.1007/s42979-024-03379-y.
9. Malerba M, Cerana R. Chitosan effects on plant systems. Int J Mol Sci. 2016;17:996. 10.3390/ijms17070996.
10. Montalvo D, Degryse F, da Silva RC, McLaughlin MJ. López-Vicente, M. Agronomic effectiveness of zinc sources as micronutrient fertilizer. Adv Agron. 2016;139:215–67.
11. Olanrewaju OS, Glick BR, Babalola OO. Mechanisms of action of plant growth promoting bacteria. World J Microbiol Biotechnol. 2017;33:197. 10.1007/s11274-017-2364-9.
12. Raza A, et al. Impact of climate change on crops adaptation and strategies to tackle its outcome: A review. Plants. 2019;8:34. 10.3390/plants8020034.
13. Sadeghi-Tehran P, Sabermanesh K, Virlet N, Hawkesford MJ. Automated method to determine two critical growth stages of wheat: heading and flowering. Front Plant Sci. 2017;8:252. 10.3389/fpls.2017.00252.
14. Shang Y, et al. Applications of nanotechnology in plant growth and crop protection: A review. Molecules. 2019;24:2558. 10.3390/molecules24142558.
15. Tisné S, et al. Phenoscope: an automated large-scale phenotyping platform. New Phytol. 2013;199:602–15. 10.1111/nph.12284.
16. Trivedi P, et al. Plant-microbiome interactions: from community assembly to plant health. Nat Rev Microbiol. 2020;18:607–21. 10.1038/s41579-020-0412-1.
17. Walter A, et al. Plant phenotyping: from bean weighing to image analysis. Plant Methods. 2020;16. 10.1186/s13007-020-00606-4.

Figures

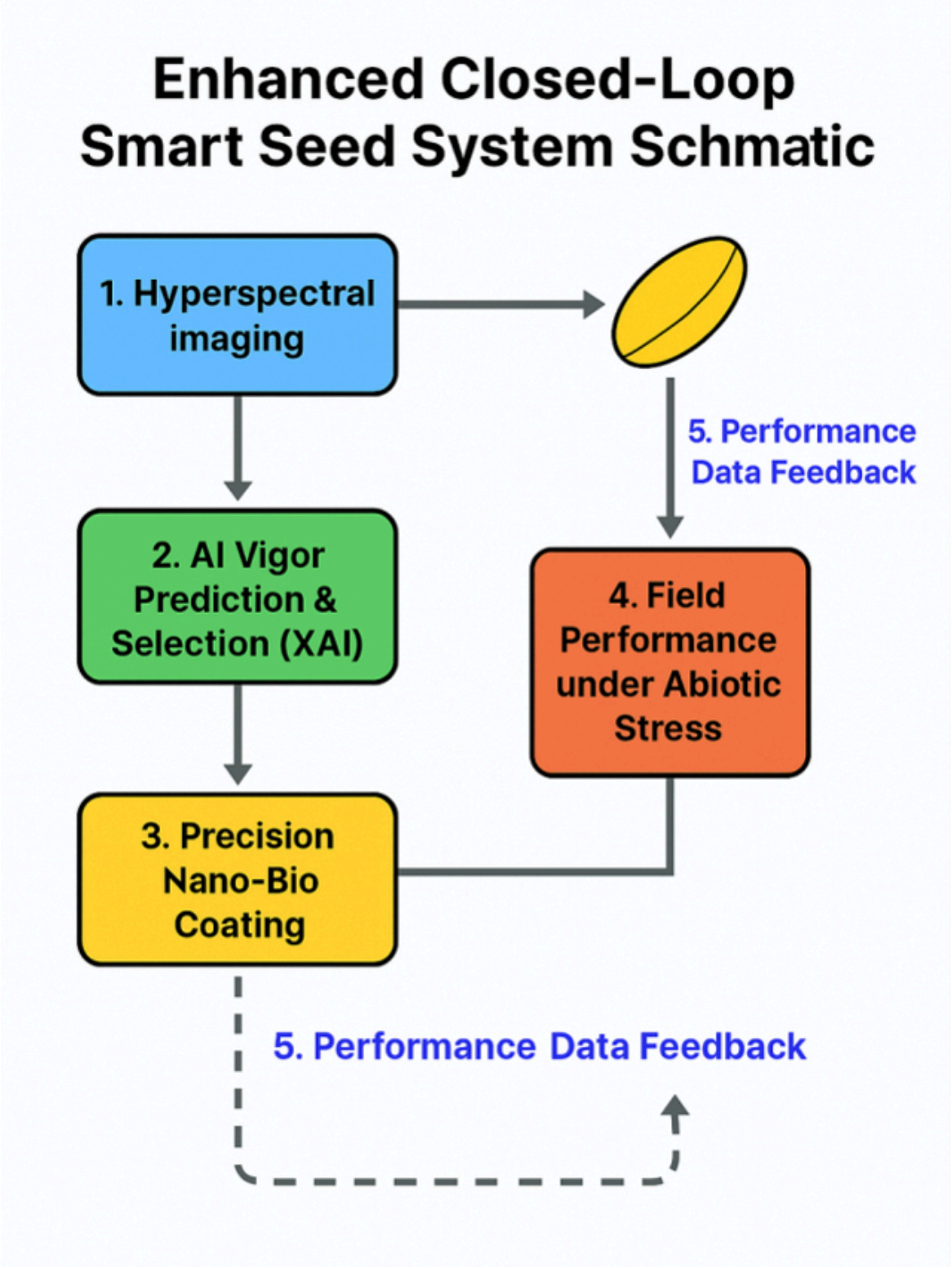

Figure 1

Agronomic performance data from controlled drought experiments can be fed back to further refine the AI model, completing the loop.

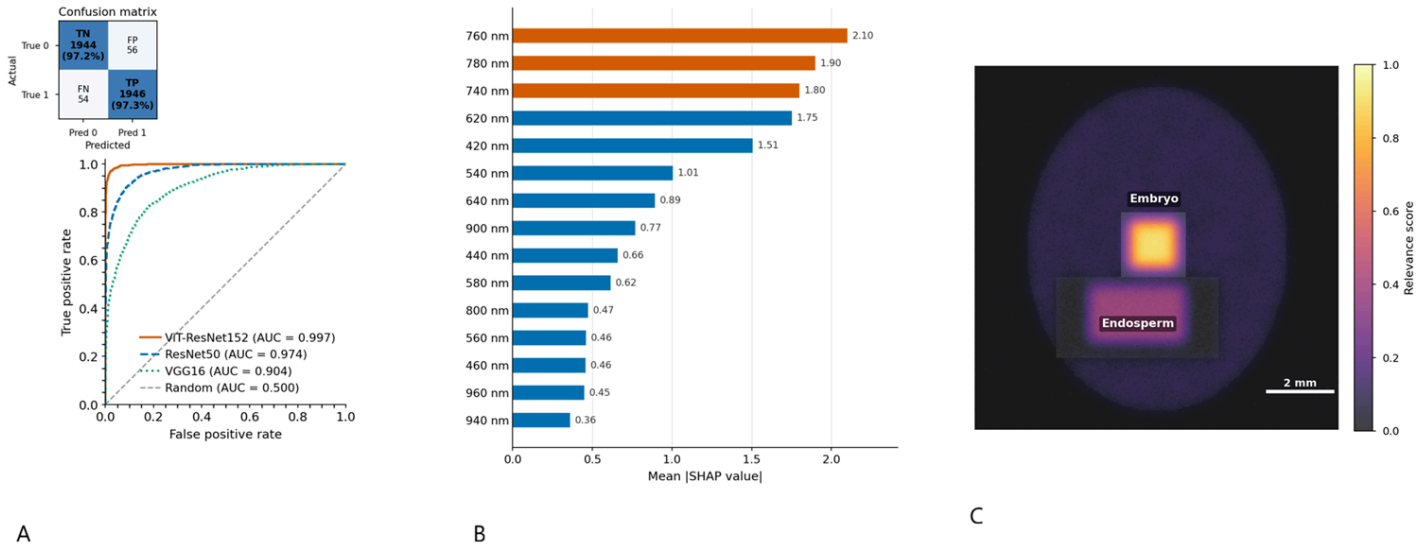

Figure 2

a. Receiver operating characteristic (ROC) curves for seed vigor prediction. The hybrid ViT-ResNet152 model (solid orange, AUC = 0.993, 95% CI: 0.989–0.997) outperforms ResNet50 (dashed blue, AUC = 0.974), VGG16 (dotted green, AUC = 0.904), and a random classifier (dashed black, AUC = 0.500). Performance metrics were computed on the independent external validation set (n = 4,000 seeds). Inset: confusion matrix showing true positive rate (96.5%) and true negative rate (98.2%)**.**

b. SHAP summary plot of the top 15 spectral features. Wavelengths in the near-infrared region (760–780 nm) show the highest mean absolute SHAP values, indicating their strong contribution to seed vigor prediction. These wavelengths correspond to water-binding capacity and starch conformation.

c. Layer-wise Relevance Propagation (LRP) heat map. Warmer coolers (red/yellow) indicate regions of the seed image that contributed most to the model's high-vigor classification. The model focuses on the embryo axis and seed coat, which are physiologically relevant for vigor assessment.

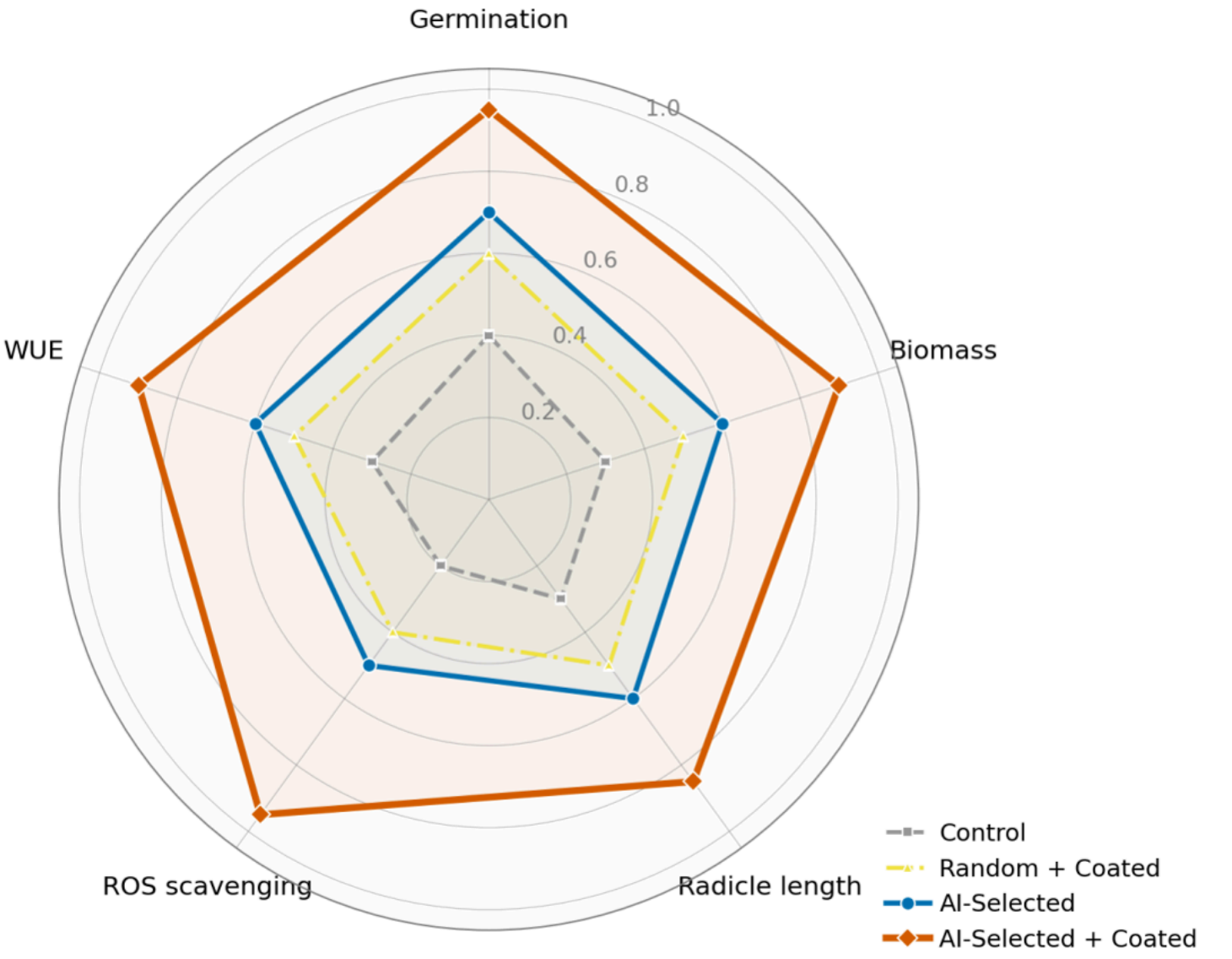

Figure 3

Multi-parameter performance profile under drought stress. Radar chart comparing the four treatment groups across five metrics (normalized 0–1 scale): germination percentage, seedling dry biomass, radicle length, ROS scavenging capacity (estimated from antioxidant enzyme activity), and water use efficiency (WUE). The AI-Selected + Coated group (red) shows the largest polygon area, indicating superior and balanced performance. Other groups: Control (grey), Random + Coated (yellow), AI-Selected + Uncoated (blue).

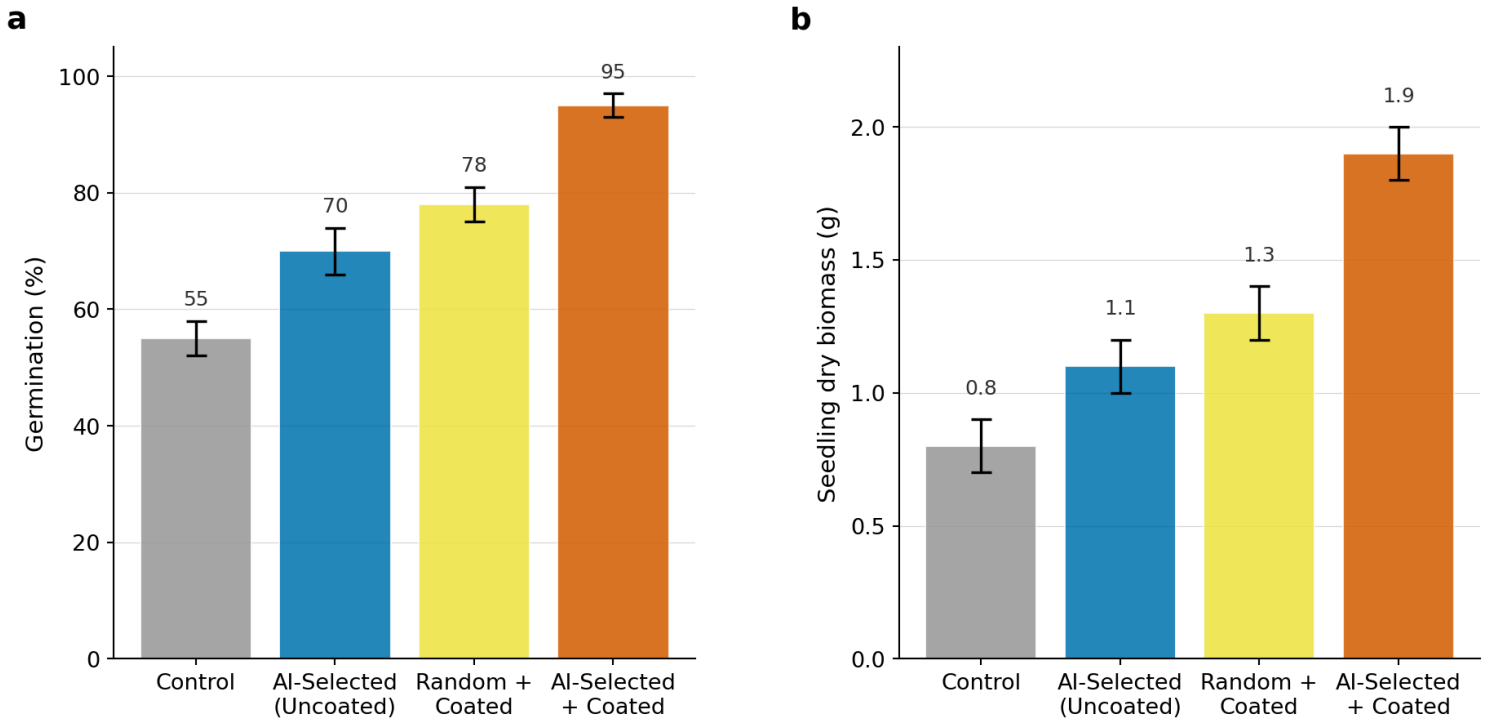

Figure 4

Agronomic performance under progressive drought stress. (a) Final germination percentage and (b) seedling dry biomass for the four treatment groups. Data are mean ± SEM (n=3 biological replicates, 50 seeds each). Different letters above bars indicate significant differences ($p < 0.05$, Tukey's HSD test). The AI-Selected + Coated group outperforms all others, confirming a synergistic interaction between AI selection and Nano-bio coating.

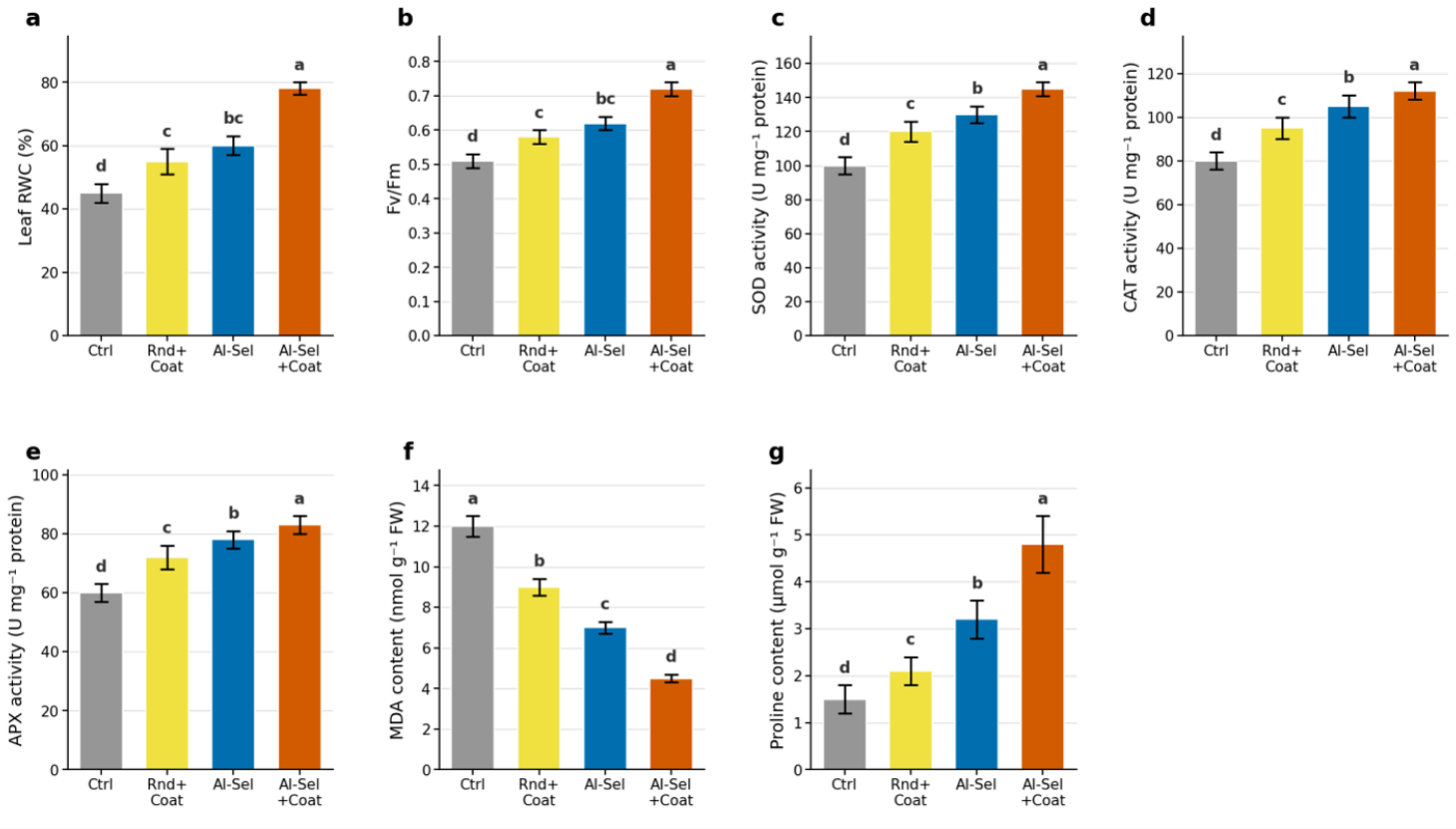

Figure 5

Physiological and biochemical responses to drought stress. (a) Leaf relative water content (RWC), (b) chlorophyll fluorescence (Fv/Fm), (c) SOD activity, (d) CAT activity, (e) APX activity, (f) MDA content as a marker of oxidative damage, and (g) proline content. Data are mean ± SEM (n=3). Asterisks indicate significant differences compared to control (*p < 0.05, **p < 0.01, ***p < 0.001). The Al-Selected + Coated group shows enhanced water retention, photosynthetic efficiency, antioxidant capacity, and osmo-protectant accumulation.

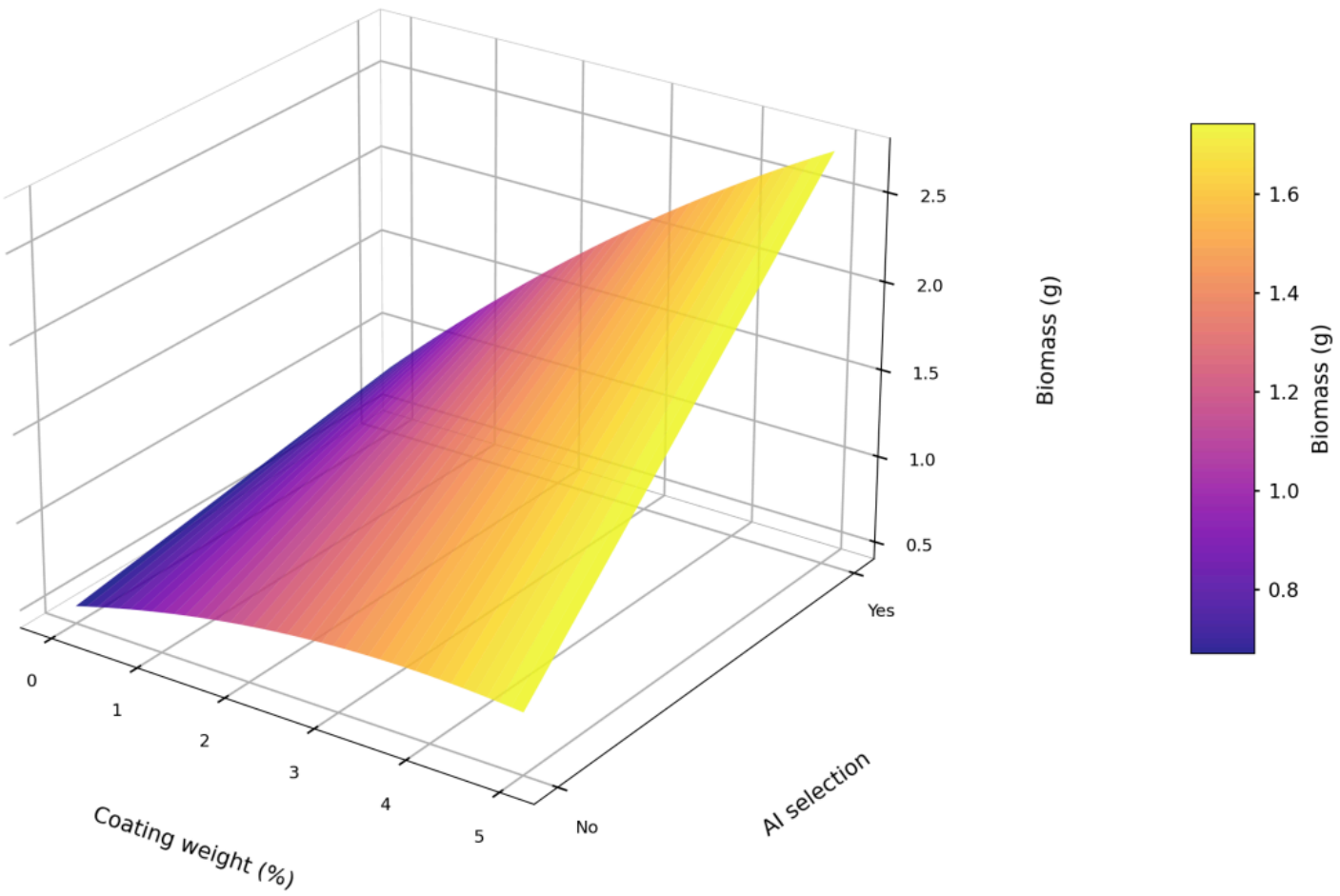

Figure 6

Response surface methodology (RSM) for seedling dry biomass. The surface models biomass as a function of AI selection (categorical: 0 = no, 1 = yes) and coating weight (continuous, 0–5%). The positive curvature and non-parallel contours indicate a significant synergistic interaction (AI × Coating, p = 0.0003). The optimal coating weight is approximately 3.72% (w/w), beyond which biomass gains diminish.

Supplementary Files

This is a list of supplementary files associated with this preprint. Click to download.

- Highlights.docx
- SupplementaryFigureS1.docx